POSITION-PATCH BASED FACE HALLUCINATION VIA LOCALITY-CONSTRAINED REPRESENTATION

Junjun Jiang, *Ruimin Hu*, *Zhen Han*, *Tao Lu*, *and Kebin Huang*

National Engineering Research Center for Multimedia Software, School of Computer, Wuhan University, Wuhan, 430072, China
{jiangjunjun, hrm1964, hanzhen, lut, kebin_huang}@whu.edu.cn

ABSTRACT

Instead of using probabilistic graph based or manifold learning based models, some approaches based on *position-patch* have been proposed for face hallucination recently. In order to obtain the optimal weights for face hallucination, they represent image patches through those patches at the same position of training face images by employing least square estimation or convex optimization. However, they can hope neither to provide unbiased solutions nor to satisfy locality conditions, thus the obtained patch representation is not the best. In this paper, a simpler but more effective representation scheme— *Locality-constrained Representation* (LcR) has been developed, compared with the Least Square Representation (LSR) and Sparse Representation (SR). It imposes a *locality constraint* onto the least square inversion problem to reach sparsity and locality simultaneously. Experimental results demonstrate the superiority of the proposed method over some state-of-the-art face hallucination approaches.

Index Terms— face hallucination, super-resolution, Locality-constrained Representation, position-patch

1. INTRODUCTION

Learning-based face image super-resolution, referred as face hallucination, has attracted numerous heed of researchers [1]. The availability of high-resolution (HR) face image, which basically means that it is reproduced with a high level of detail, allows many applications, such as robust face recognition, 3D facial modeling and Intelligent Video Surveillance. Employing a training set of face images, the face hallucination technology could generate a HR face image from a low-resolution (LR) one. By building a co-occurrence model, the missing details of the input LR face image could be made up globally (global face space parameter estimation, e.g., [3],[11]), locally (local image primitive intensity restoration, e.g., [1],[5],[6],[7],[9],[10]), or both (e.g., [2],[8]). Since the local patch based methods can greatly improve the quality of hallucinated faces, they gain much more concern in the super-resolution research community.

Inspired by the results of face analysis that human face is a class of highly structured object and consequently position plays an increasingly important role in its reconstruction, some position-patch based face hallucination methods have been proposed. The key issue of those methods is how to represent the image patch and obtain the optimal weight vector (Fig.1). For example, Ma *et al.* [6-7] employ patches at same position of all training face images to hallucinate the HR image patch through solving a least square problem. Due to reasonable utilization of position information, it is more efficient and the performance is excellent, compared with some manifold learning based methods [4]. However, when the number of the training samples is much larger than the dimension of the patch, the solution of least square estimation is not unique [8]. In order to solve the biased solutions, Jung *et al.* [9] take a convex constrained optimization to replace the least square estimation to obtain more suitable solution. However, it overemphasizes the sparsity and neglects the locality condition, which is more important than sparsity in revealing the non-linear manifold structure of face image patch space [12-13]. Thus, the obtained patch representation is still not the best. Since the local image patches share the greatest similarity, it would be more accurate to represent one image patch using a few neighbor patches, leading to a more effective representation of image patches.

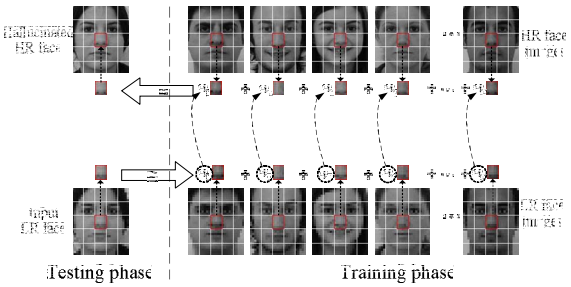

Fig.1. Flow diagram of the position-patch based face hallucination framework. To obtain the optimal weight vector $w=[w_1, w_2, \cdots, w_M]$ is the key issue.

Contribution. In this paper, we introduce a novel patch representation method for face image hallucination, called Locality-constrained Representation (LcR) which imposes a locality constraint onto the least square inversion problem. Instead of representing one input image patch collaboratively [6-7] or sparsely [8-9], we utilize the locality constraint to project each image patch into its several neighborhoods, thus achieving sparsity and locality

978-0-7695-4711-4/12 $26.00 © 2012 IEEE
DOI 10.1109/ICME.2012.152

simultaneously. There are three characteristics of the proposed method:

(1) By introducing a locality constraint, it makes the solution of the least square problem fixed, meanwhile it captures fundamental similarities between neighbor patches;

(2) Compared with traditional locality preserving methods that use a fixed number of neighbors for reconstruction, it chooses the most relevant patches adaptively to avoid over- or under-fitting, generating sharper contours and richer details;

(3) While sparse representation methods must solve the ℓ^1-norm constrained minimization problem, it derives an analytical solution to the constrained least squares problem, significantly reducing the computational complexity.

The rest of this paper is organized as follows. Section 2 briefly reviews LSR, SR and then presents our LcR method. Section 3 describes the proposed face hallucination method based on LcR. Experimental results and analyses are provided in Section 4, and we conclude this paper in Section 5.

2. LOCALITY-CONSTRAINED REPRESENTATION

This section reviews two existing patch representation schemes, LSR and SR, and introduces our proposed LcR method.

Let Y^m denote the training face images, $m = 1,...,M$, where M is the sample number. Each face image is divided into N small overlapping patch sets $\{Y^m(i,j) \mid 1 \le i \le U, 1 \le j \le V\}$, $N = UV$, U represents the patch number in every column, V represents the patch number in every row, and the term (i,j) indicates the position information (as illustrated in Fig.2). For the patch located at position (i,j), it can be represented by M training samples located at the same position with a weight vector, $w(i,j) = [w_1(i,j), w_2(i,j), ..., w_M(i,j)]$.

For one input face image denoted in patches as $\{X(i,j) \mid 1 \le i \le U, 1 \le j \le V\}$, different representation schemes convert each patch into a M-dimensional optimal weight vector to generate the final patch representation.

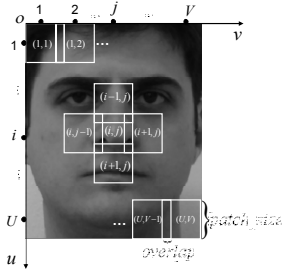

Fig.2. Dividing a face into $N=UV$ patches. The term (i, j) indicates the coordinate of one patch in the patch coordinate system o-uv. *patch_size* and *overlap* denote the side pixels of one square patch and the overlap pixels between patches respectively.

2.1. Least Square Representation

LSR [6-7] uses patches from all training samples at the same position (i,j) to represent one patch $X(i,j)$:

$$X(i,j) = \sum_{m=1}^{M} w_m(i,j) Y^m(i,j) + e \tag{1}$$

where e is the reconstruction error.

The optimal weight can be solved by the following constrained least square fitting problem:

$$w^*(i,j) = \arg\min_{w(i,j)} \| X(i,j) - \sum_{m=1}^{M} w_m(i,j) Y^m(i,j) \|_2^2 \quad s.t. \sum_{m=1}^{M} w_m(i,j) = 1 \tag{2}$$

where $w^*(i,j) = [w_1(i,j), w_2(i,j), ..., w_M(i,j)]$ is the optimal M- dimensional weight vector for $X(i,j)$.

2.2. Sparse Representation

In practice, the solution $w(i,j)$ to equation (2) may not unique and a possible way is to impose several regularization terms onto it.

Jung *et al.* [9] introduce the *Sparse Representation* theory and use a small subset of patches to represent $X(i,j)$ instead of performing collaboratively over the whole training samples. It converts equation (2) to a standard sparse representation problem:

$$\min \| w(i,j) \|_1, \quad s.t. \| X(i,j) - \sum_{m=1}^{M} w_m(i,j) Y^m(i,j) \|_2^2 \le \varepsilon \tag{3}$$

where $\| \bullet \|_1$ denotes the ℓ^1-norm. This sparsity constraint can not only ensure that the under-determined equation have an exact solution but also allow the learned representation for each patch $X(i,j)$ to capture salient properties, thus achieves much less reconstruction error.

2.3. Locality-constrained Representation

The work in [9] emphasizes that a strong sparsity of the weight vector $w(i,j)$ is important in representing the input patch but it doesn't investigate much the role of a locality constraint, which is more essential than sparsity in revealing the true geometry of a nonlinear manifold [12-13]. In other words, SR might represent one input patch by training data from distinct patches.

Following the intuition that *Local Coordinate Coding* (LCC) [12-13] could explicitly encourage the representation to be local, we incorporate a locality constraint instead of the sparsity constraint into the objective function. Additionally, we adopt shrinkage measures as in ridge regression on the weight vector $w(i,j)$. Based on the above discussions, our objective function is formulated as follows:

$$\min \| d(i,j) \circ w(i,j) \|_2^2, \quad s.t. \| X(i,j) - \sum_{m=1}^{M} w_m(i,j) Y^m(i,j) \|_2^2 \le \varepsilon \tag{4}$$

where $\circ$ denotes a point wise vector product. And $d(i,j)$ is a M-dimensional vector that penalizes the distance between $X(i,j)$ and each training patch at the same position. It is simply determined by the squared Euclidean distance:

$$d_m(i,j) = \| X(i,j) - Y^m(i,j) \|_2^2, \quad 1 \le m \le M \tag{5}$$

Equivalently, equation (4) can be written as:

$$w^*(i,j) = \arg\min_{w(i,j)} \left\{ \begin{array}{l} \| X(i,j) - \sum_{m=1}^{M} w_m(i,j) Y^m(i,j) \|_2^2 + \\ \tau \sum_{m=1}^{M} \| w_m(i,j) \circ d_m(i,j) \|_2^2 \end{array} \right\} \tag{6}$$

The above objective function consists of two parts: The first term measures the reconstruction error and the second term preserves locality in representation. τ is a regularization parameter balancing the contribution of the reconstruction error and locality of the solution. When $\tau = 0$, LcR reduces to LSR. In our method, the locality constraint has a twofold role. On one hand, it makes the solution fixed; On the other hand, it introduces a locally constrained sparse representation to each patch, yet this "sparsity" is much weaker than that in the sense of ℓ^0-norm. This will be discussed in Section 4.5.

2.4. Optimization

Following [13], the solution of a regularized least square in equation (6) can be derived analytically by:

$$w(i,j) = (G(i,j) + \tau D) \backslash 1 \tag{7}$$

where D is a $M \times M$ diagonal matrix:

$$D_{mm} = d_m(i,j), \quad 1 \le m \le M \tag{8}$$

G is local covariance matrix for $X(i,j)$ as:

$$G(i,j) = CC^T . \tag{9}$$

Define C as:

$$C = (X(i,j) \cdot ones(1,M) - Y(i,j)) \tag{10}$$

where $Y(i,j)$ is a matrix with its columns being training patches $Y^m(i,j)$, $ones(1,M)$ is a $1 \times M$ row vector of ones, and the superscript "T" means transpose. The final optimal weight is obtained by rescaling it so that $\sum_{m=1}^{M} w_m(i,j) = 1$.

3. FACE HALLUCINATION VIA LOCALITY-CONSTRAINED REPRESENTATION

The training set is composed of HR and LR face image pairs. HR face images are denoted as $\{Y_H^m\}_{m=1}^M$ and their LR counterparts are denoted as $\{Y_L^m\}_{m=1}^M$. The primary task is to reconstruct the HR face image X_H from the observed LR face image X_L.

At the beginning, we divide the training face images and the input LR face image into patches using the same dividing scheme. In order to avoid changing the size of the image because of cutting or filling, we take a "fallback" dividing strategy as illustrated in Fig.3. Therefore, the patch number in every column, *U*, and the patch number in every row, *V*, can be obtained:

$$U = \text{ceil}\left\{ \frac{imrow - overlap}{patch\_size - overlap} \right\} \tag{11}$$

Algorithm 1 Face hallucination via LcR.

1. **Input:** Training set $\{Y_H^m\}_{m=1}^M$ and $\{Y_L^m\}_{m=1}^M$, a LR image X_L, *patch_size*, *overlap* and regularization parameter τ.
2. Compute *U* and *V*:
   U = ceil((*imrow* - *overlap*)/(*patch_size* - *overlap*))
   V = ceil((*imcol* - *overlap*)/(*patch_size* - *overlap*))
3. Divide each of the training images and the input LR image into *N* small patches according to the same location of face, $\{Y_H^m(i,j) \mid 1 \le i \le U, 1 \le j \le V\}_{m=1}^M$, $\{Y_L^m(i,j) \mid 1 \le i \le U, 1 \le j \le V\}_{m=1}^M$ and $\{X_L(i,j) \mid 1 \le i \le U, 1 \le j \le V\}$, respectively.
4. **For** i = 1 to *U* **do**
5. **For** j = 1 to *V* **do**
   - Calculate the distance between the input LR image patch $X_L(i,j)$ and all the *M* training image patches $\{Y_L^m(i,j)\}_{m=1}^M$ at position (i,j):
     $$d_m(i,j) = \| X_L(i,j) - Y_L^m(i,j) \|_2^2, \quad 1 \le m \le M$$
   - Compute the optimal weight vector $w^*(i,j)$ for the input LR image patch $X_L(i,j)$ with the LR training image patches $\{Y_L^m(i,j)\}$:
     $$w^*(i,j) = \arg\min_{w(i,j)} \left\{ \begin{array}{l} \| X_L(i,j) - \sum_{m=1}^{M} w_m(i,j) Y_L^m(i,j) \|_2^2 + \\ \tau \sum_{m=1}^{M} \| w_m(i,j) \circ d_m(i,j) \|_2^2 \end{array} \right\}$$
   - Construct the HR patch by
     $$X_H(i,j) = \sum_{m=1}^{M} w_m^*(i,j) Y_H^m(i,j) .$$
6. **End for**
7. **End for**
8. Integrate all the reconstructed HR patches above according to the original position. The final HR image X_H can be generated by averaging pixel values in the overlapping regions.
9. **Output:** HR hallucinated face image X_H.

$$V = \text{ceil}\left\{ \frac{imcol - overlap}{patch\_size - overlap} \right\} \tag{12}$$

where *imrow* and *imcol* denote the rows and columns of a face image, respectively, ceil(*x*) is the function that rounds the elements of *x* to the nearest integers towards infinity.

For each input LR patch image, by imposing locality constraint onto the objective function, the representation can achieve not only locality but also sparsity. The entire face hallucination process is summarized in Algorithm1.

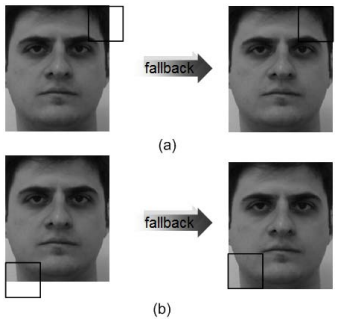

Fig.3. Illustration of the "fallback" dividing strategy. (a) When the current patch slid off the right edge, let it fallback subject to the right edge; (b) when the current patch slid off the bottom edge, let it fallback subject to the bottom edge.

4. EXPERIMENT RESULTS

4.1. Database

In the experiments, we use the frontal and pre-aligned images of FEI Face Database[1] [14]. The database contains 400 images from 200 subjects (100 men and 100 women) and each subject has two frontal images, one with a neutral expression and the other with a smiling facial expression. Human faces in the database are mainly from 19 and 40 years old with distinct appearances, hairstyles and adornments (Fig.4). All the images are cropped to 120×100 pixels, and we choose 360 images (180 subjects) as the training set, leaving the rest 40 images (20 subjects) for testing. Therefore, all the test images are not in the training set. The LR images are formed by smoothing (an averaging filter of size 4×4) and down-sampling (by a factor of 4, thus the size of LR face images are 30×25 pixels) from corresponding HR images.

Fig.4. Some training faces in FEI Face Database.

4.2. Parameter Settings

We compare the proposed method with Wang's eigentransformation method [3] and some patch based methods, such as Chang's Neighbor Embedding method [4], Ma's LSR method [7] and Jung's SR method [9], under FEI Face Database. In order to obtain the best performance, we adjust the parameters for each comparative method. For Wang's eigentransformation method, we let the variance accumulation contribution rate of PCA be 98.5% (around 100 bases). For the sake of fair competition, we set the HR patch size to 12×12 in Chang's Neighbor Embedding method, LSR, SR and our LcR method and the overlap between neighbor patches is 4 pixels while corresponding LR image patch size is set to 3×3 with overlap of 1 pixel. In the experiments, we find that the more overlap the better the final result is. Obviously, the more overlap the longer the running time is. Therefore, we must balance performance and efficiency. The number of neighbors in Chang's Neighbor Embedding is set to 50. For Jung's SR method, we set error tolerance to 1.0 and use a primal-dual algorithm [16] for sparse representation problem as in their method. Our algorithm has only one free parameter τ. In our experience, τ is set to 0.04 and we will demonstrate the performance versus the value of τ in Section 4.4.

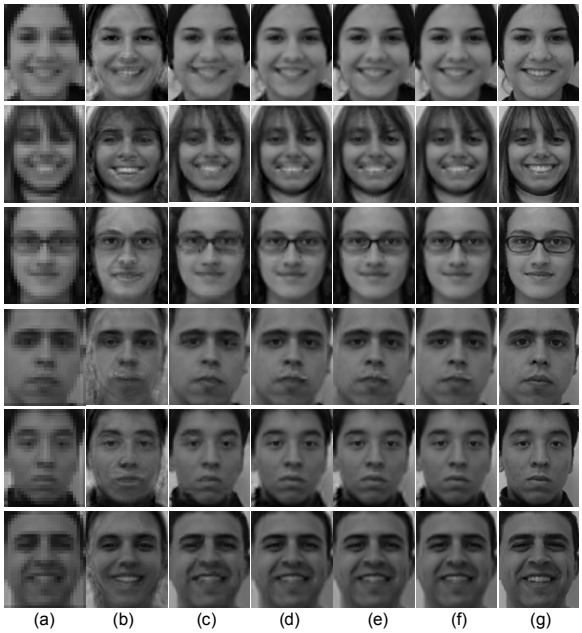

Fig.5. Comparison of results based on different methods. (a) Input LR faces. (b) Wang *et al*. [3]. (c) Chang *et al*. [4] (d) Ma *et al*. [7] (e) Jung *et al*. [9] (f) Our method. (g) Original HR faces. (Note that the effect is more pronounced if the figure of the electronic version is zoomed.).

4.3. Results

The experimental results are shown in Fig.5. Due to space limitation, we don't provide all the results here. We can observe that **(1)** Patch based methods outperform global faces reconstruction methods. In Wang's eigentransformation method, it hardly maintains global smoothness but also leads to "ghost" artifacts around contour. Compared with that, patch based methods show their superiority and further enhance the edges and textures. This is mainly because Wang's method is based on a statistical mode, which could not reveal the distribution of data when the training samples are not sufficient (e.g., 360 training samples in our experiments while the feature dimension is 30×25 = 750); **(2)** Position-patch based methods are better than Chang's Neighbor Embedding based patch method [4]. From Fig.5 (c), we can see that the hallucinated face images by Chang's method have blurring effects, primarily due to over or under-fitting. In addition, by using the position information of human faces in face reconstruction, position-patch based methods capture the latent semantic information (e.g., patch position), while Chang's method considers only the aspect of reconstruction and ignores the semantic features of faces; **(3)** A further examination shows that our method successfully captures more high frequency components and fewer artifacts than Ma and Jung's position-patch based methods (see the mouth of 2-th row, the edge of 3-th row and the face contours of 5-th and 6-th rows in Fig.5). The excellent visual quality of our method owes to the LcR strategy; **(4)** The PSNR

[1] It is publicly available on http://fei.edu.br/~cet/facedatabase.html

and SSIM [2][15] by different methods are shown in box--plots in Fig.6. Again, we can see that our method gives higher PSNR and SSIM values than those of other four methods. Specifically, the average PSNR and SSIM improvements of LcR based face hallucination method over the second best method (i.e., Jung's SR based method [9]) are 0.65 dB and 0.0097, respectively.

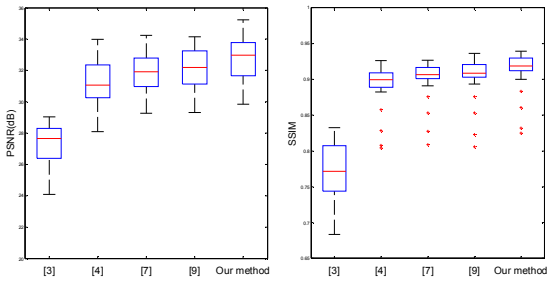

Fig.6. PSNR (left) and SSIM (right) competitions of different methods. The average PSNR and SSIM of different methods: [3] (PSNR = 27.26, SSIM = 0.7684), [4] (PSNR = 31.26, SSIM = 0.8944), [7] (PSNR = 31.90, SSIM = 0.9032), [9] (PSNR = 32.11, SSIM = 0.9048) and our method. (PSNR = **32.76**, SSIM = **0.9145**).

4.4. The Performance of Different τ

Additionally, we test the performance of our method by choosing different regularization parameter τ, which controls the weights of locality in the objective function. As shown in Fig.7, we can find that when $\tau = 0$, which can be regarded as the same case of LSR, the performance of LcR is not the best. With the increase of locality, much benefit on performance can be gained. This implies that the locality constrain is essential for patch reconstruction. However, we also should see that the value of τ could not be set too high because the reconstruction error in the objective function can not be ignored also. Therefore, selecting a proper regularization parameter τ, LcR will gain good results.

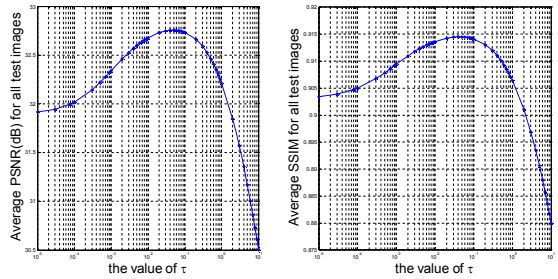

Fig.7. The average PSNR and SSIM values versus different τ.

4.5. The Sparsity of LcR

To get a better understanding of our approach, we plot the connected optimal weight vector, which is formed by connecting the optimal weight vectors $w(i,j)$ of each patch of all 40 test images, for different representation methods (Fig.8). The plots show that reconstruction weight vector under LSR is not sparse for it treats all the samples indifferently. Our LcR obtains a sparse result to some extent when compared with SR. And it allows us to ensure that LcR can truly reveal the image space, which is embedded in a nonlinear manifold [4]. At the same time, we also find an encouraging phenomenon. The weights obtained by LSR and SR are equably distributed on both sides of zero, while LcR gains a non-negative reconstruction weights (most values are higher than zero as shown in the bottom left of Fig.8). This phenomenon can be easily explained—if we use several neighbor patches of one image patch to represent it, each image patch should have a positive contribution.

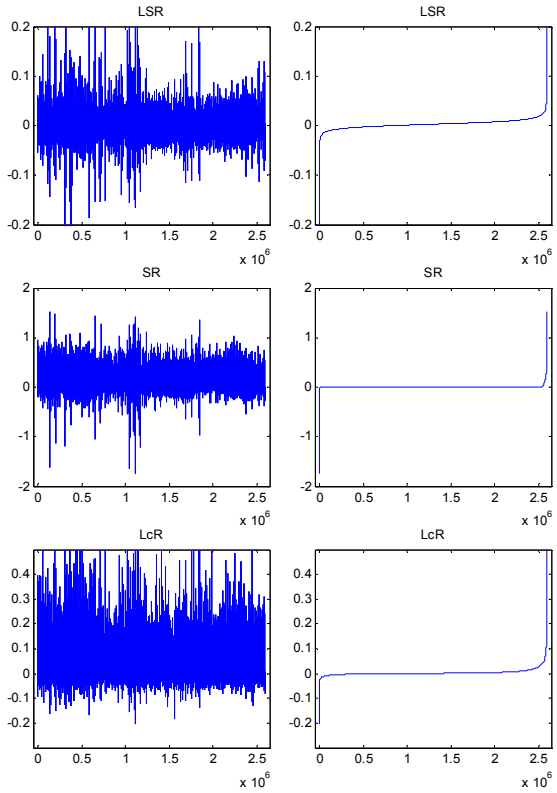

Fig.8. The sparsity of the connected optimal weight vector for different representation methods (Top row: LSR, Middle row: SR, Bottom row: LcR). The left figures are the plots of the connected optimal weight vector and the right figures are the plots of sorted connected optimal weight vector.

4.6. The locality of LcR

In this subsection, we will check the locality of LSR, SR and LcR, respectively. At the beginning, we define an evaluation metric of locality, which called *K-mean distance* (*K*-MD). Denote $X(i,j)$ as the inference patch and $\{Y^k(i,j) \mid k \in C(K)\}$ as the *K most significant* patches in training samples at the same position (i,j) and $C(K)$ are their sample indexes. The larger the entries in the weight vector $w(i,j)$, the more important the corresponding patch.

[2] The higher the SSIM value, the better is the face hallucination quality. The maximum value of SSIM is 1, which means a perfect reconstruction.

K-MD is defined as:

$$K\text{-MD}(i,j)=\left\{\frac{\sum_{k\in C(K)}\| X(i,j)-Y^{k}(i,j)\|_2^2}{K}\right\}^{\frac{1}{2}} \qquad (13)$$

From the definition of K-MD, we learn that it measures the locality of a representation approach by computing the distance between the inference patch and K largest weight patches in the representation of the inference patch. Therefore, a small K-MD indicates better preservation of locality. If the value of K-MD is high, it will choose very distinct patches as the base, which is not consistence with the common sense. The evaluation of locality of LSR, SR and LcR is given in Fig.9. From this comparison, we can clearly see that LcR can better capture the locality property than LSR and SR.

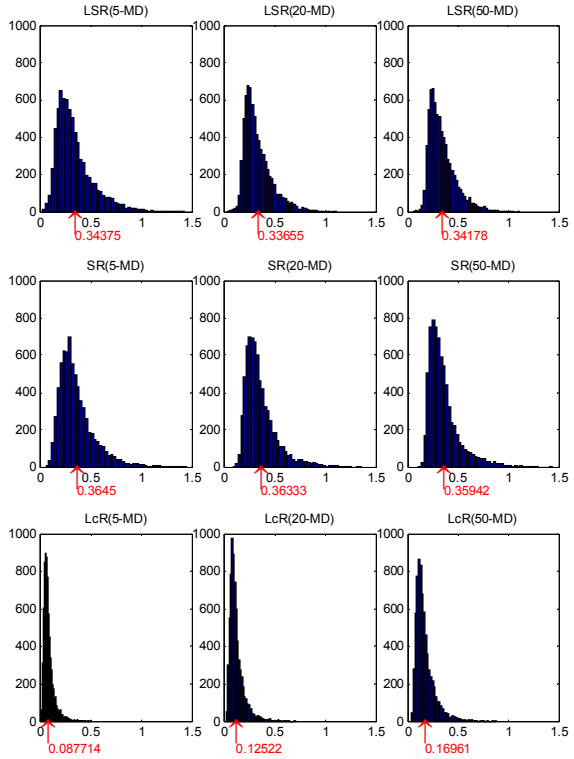

Fig.9. Histograms of the K-mean distance for different methods when K = 5, 20, 50, respectively. (Top row: LSR, Middle row: SR, Bottom row: LcR). The red arrows indicate the median values.

5. CONCLUSION AND FUTURE WORK

In this paper, we have proposed a novel patch representation algorithm, called *Locality-constrained Representation* (LcR), for face hallucination. It imposes a *locality constraint* rather than *sparsity constraint* onto least square inversion problem, aiming at obtaining the optimal representation of one image patch. In this method, each patch can be represented by a small number of bases, which are adaptively selected from its neighborhoods, thus achieving sparsity and locality simultaneously. Experimental results on the same database have demonstrated the superiority of the proposed method over some state-of-the-art methods. Nonetheless, we set the regularization parameter τ experimentally, the impact of noise and the regularization parameter τ on the proposed LcR method needs further work.

6. ACKNOWLEDGMENTS:

The research was supported by the major national science and technology special projects (2010ZX03004-003-03), the National Basic Research Program of China (973 Program) (2009CB320906), the National Natural Science Foundation of China (61172173, 60832002, 60970160, 61070080, 61003184), the National Science Foundation of Hubei Province of China (2010CDB05103), the Fundamental Research Funds for the Central Universities (201121102020009, 3101011), the science and technology Program of Wuhan (201271031366).

7. REFERENCES

[1] K. Jia and S. Gong, "Generalized Face Super-Resolution," *IEEE Trans. Image Process.* , vol.17, no.6, pp.873–886, 2008.

[2] C. Liu, H. Shum, and W. Freeman, "Face hallucination: Theory and practice," *Int. J. Comput. Vis.*, vol.7, no.1, pp.115–134, 2007.

[3] X. Wang and X. Tang, "Hallucinating face by eigen-transformation," *IEEE Trans. Systems, Man, and Cybernetics. Part C*, vol.35, no.3, pp.425–434, 2005.

[4] H. Chang, D. Yeung, and Y. Xiong, "Super-resolution through neighbor embedding," in *Proc. IEEE Conf. Computer Vision and Pattern Recognition*, pp. 275–282, 2004.

[5] B. Li, H. Chang, S. Shan and X. Chen, "Aligning Coupled Manifolds for Face Hallucination," *IEEE Signal Process. Lett.*, vol.16, no.11, pp.957–960, 2009.

[6] X. Ma, J. Zhang, and C. Qi, "Position-based face hallucination method," in *Proc. IEEE Conf. Multimedia and Expo.*, pp.290–293, 2009.

[7] X. Ma, J. Zhang, and C. Qi, "Hallucinating face by position-patch," *Pattern Recognition*, vol.43, no.6, pp.3178–3194, 2010.

[8] J. Yang, H. Tang, Y. Ma, and T. Huang, "Face hallucination via sparse coding," in *Proc. IEEE Conf. Image Process.*, pp.1264–1267, 2008.

[9] C. Jung, L. Jiao, B. Liu, and M. Gong, "Position-Patch Based Face Hallucination Using Convex Optimization," *IEEE Signal Process. Lett.*, vol.18, no.6, pp.367–370, 2011.

[10] X. Ma, H. Huang, S. Wang, and C. Qi, "A simple approach to multiview face hallucination," *IEEE Signal Process. Lett.*, vol.17, no.6, pp.579–582, 2010.

[11] J. Park and S. Lee, "An example-based face hallucination method for single-frame, low-resolution facial images," *IEEE Trans. Image Process.*, vol.17, no.10, pp.1806–1816, 2008.

[12] K. Yu, T. Zhang, and Y. Gong, "Nonlinear learning using local coordinate coding," *in Proc. of Advances in Neural Information Processing Systems,* pp.2223-2231, 2009.

[13] J. Wang, J. Yang, K. Yu, F. Lv, T. Huang, and Y. Gong, "Locality-constrained Linear Coding for Image Classification," in *Proc. IEEE Conf. Computer Vision and Pattern Recognition*, pp.3360–3367, 2010.

[14] C. Thomaz, G. Giraldi, "A new ranking method for principal components analysis and its application to face image analysis," *Image and Vision Computing*, vol.28, no.6, pp.902–913, 2010.

[15] Z. Wang, A. Bovik, H. Sheikh, and E. Simoncelli, "Image quality assessment: From error visibility to structural similarity," *IEEE Trans. Image Process.* , vol.13, no.4, pp.600–612, 2004.

[16] E. Candes and J. Rombergt, ℓ^1-Magic: Recovery of Sparse Signals via Convex Programming 2005 [Online]. Available: http://www.acm.caltech.edu/l1magic/